THE JOURNAL OF BIOLOGICAL CHEMISTRY VOL. 286, NO. 39, pp. 34413–34425, September 30, 2011

Antidepressant-induced Ubiquitination and Degradation of the Cardiac Potassium Channel hERG*[S]

Received for publication, April 23, 2011, and in revised form, July 30, 2011 Published, JBC Papers in Press, August 9, 2011, DOI 10.1074/jbc.M111.254367

Adrienne T. Dennis[‡], Drew Nassal[‡§], Isabelle Deschenes[‡§], Dierk Thomas[¶], and Eckhard Ficker[‡1]

From the [‡]Rammelkamp Center for Education and Research, MetroHealth Campus, Case Western Reserve University, Cleveland Ohio 44109, the [§]Department of Physiology and Biophysics, Case Western Reserve University, Cleveland Ohio 44106, and the [¶]Department of Cardiology, Medical University Hospital Heidelberg, D-69120 Heidelberg, Germany

Background: Acquired long QT syndrome is usually precipitated by direct hERG block.
Results: Tricyclic antidepressants do not only block hERG but inhibit forward trafficking and promote endocytosis via increased channel ubiquitination.
Conclusion: Tricyclic antidepressants trigger multiple mechanisms controlling hERG surface expression.
Significance: A better mechanistic understanding of acquired long QT syndrome impacts how cardiac safety of therapeutic compounds is assessed.

The most common cause for adverse cardiac events by antidepressants is acquired long QT syndrome (acLQTS), which produces electrocardiographic abnormalities that have been associated with syncope, torsade de pointes arrhythmias, and sudden cardiac death. acLQTS is often caused by direct block of the cardiac potassium current I_{Kr}/hERG, which is crucial for terminal repolarization in human heart. Importantly, desipramine belongs to a group of tricyclic antidepressant compounds that can simultaneously block hERG and inhibit its surface expression. Although up to 40% of all hERG blockers exert combined hERG block and trafficking inhibition, few of these compounds have been fully characterized at the cellular level. Here, we have studied in detail how desipramine inhibits hERG surface expression. We find a previously unrecognized combination of two entirely different mechanisms; desipramine increases hERG endocytosis and degradation as a consequence of drug-induced channel ubiquitination and simultaneously inhibits hERG forward trafficking from the endoplasmic reticulum. This unique combination of cellular effects in conjunction with acute channel block may explain why tricyclic antidepressants as a compound class are notorious for their association with arrhythmias and sudden cardiac death. Taken together, we describe the first example of drug-induced channel ubiquitination and degradation. Our data are directly relevant to the cardiac safety of not only tricyclic antidepressants but also other therapeutic compounds that exert multiple effects on hERG, as hERG trafficking and degradation phenotypes may go undetected in most preclinical safety assays designed to screen for acLQTS.

Drug-induced or acquired long QT syndrome (acLQTS)[2] poses a major problem for therapeutic drug use as well as for the development of novel drug compounds, as acLQTS produces electrocardiographic abnormalities that have been associated with syncope, torsade de pointes arrhythmias, and sudden cardiac death (1). In most instances, acLQTS can be traced to a well understood phenomenon; that is, direct block of the cardiac potassium current I_{Kr}/hERG, that is crucial for terminal repolarization in human heart (2). However, therapeutic compounds such as arsenic trioxide, which is used in the treatment of leukemia (3), or pentamidine, which is used in the treatment of *Pneumocystis carinii* pneumonia (4, 5), precipitate acLQTS via an unconventional mechanism; that is, drug-induced hERG trafficking inhibition (6). Moreover, up to 40% of all direct hERG-blockers combine conventional hERG block with unconventional hERG trafficking inhibition, *i.e.* they exert combined hERG activity (7–11). Few of these compounds have been fully characterized at the cellular level. This is a crucial omission, because hERG trafficking inhibition may be missed in preclinical safety assays that have been designed exclusively for the detection of direct hERG block (12).

Tricyclic and tetracyclic antidepressants (TCA) such as maprotiline, amoxapine, imipramine, or desipramine represent a large compound class with combined hERG activity that is notorious for its association with acLQTS (7, 13). TCAs have also been linked to increased risk of sudden cardiac death, especially after overdosing or with dosing regimens designed to achieve high therapeutic levels (14). Although TCAs have been somewhat supplanted by better tolerated serotonin reuptake inhibitors (SRIs), they are still widely prescribed in patients who do not tolerate SRIs or for certain off-label indications including panic disorder, migraine headaches, neuropathic pain, or

* This work was supported, in whole or in part, by National Institutes of Health Grants T32HL105338 (to D. N.) and 1R01HL096962 (to I. D.). This work was also supported in part by research grants from the Deutsche Forschungsgemeinschaft (FRONTIERS program, the ADUMED foundation, and the German Heart Foundation/German Foundation of Heart Research (all to D. T.).
[S] The on-line version of this article (available at http://www.jbc.org) contains supplemental Figs. 1–7.
[1] To whom correspondence should be addressed: Rammelkamp Center, MetroHealth Medical Center, 2500 MetroHealth Dr., Cleveland, OH 44109. Tel.: 216-778-8977; Fax: 216-778-8282; E-mail: eficker@metrohealth.org.

[2] The abbreviations used are: acLQTS, drug-induced or acquired long QT syndrome; bEAG, bovine ether a-go-go; hERG, human ether a-go-go-related gene; I_{Kr}, rapidly activating delayed rectifier K^+ current; MESNA, sodium 2-mercaptoethanesulfonate; NRVM, neonatal rat ventricular myocytes; TCA, tri- and tetracyclic antidepressants; cg, core-glycosylated; fg, fully glycosylated; desip, desipramine; ER, endoplasmic reticulum; RT, room temperature; pF, picofarads.

eating disorders (15–18). The cardiotoxicity of TCAs has been explained in many instances by acute block of I_{Kr}/hERG channels (13, 19, 20). In contrast, we have previously described desipramine-induced hERG trafficking defects (IC_{50}, 7.5 μM) in addition to conventional channel block (IC_{50}, 11.9 μM at RT) (11, 21) at concentrations within the upper therapeutic range of 3–4 μM (22). Importantly, desipramine-related safety concerns are reflected in a large number of reports of QT interval prolongation, torsade de pointes tachycardia, and sudden cardiac death (23–28). In fact, the Food and Drug Administration issued new warnings for desipramine (Norpramin®) in 2009, stating ," . . . extreme caution should be used when this drug is given to patients who have a family history of sudden death, cardiac dysrhythmias, and cardiac conduction disturbances and that seizures precede cardiac dysrhythmias, and death in some patients."

The overall goal of the present study is to understand at the cellular and molecular level how hERG surface expression is disrupted by desipramine. We address two major questions; 1) is endocytic internalization and recycling of hERG altered in the presence of desipramine? and 2) is hERG forward trafficking from the endoplasmic reticulum (ER) to the cell surface inhibited by desipramine? Our results provide a more complete mechanistic picture of the multiple effects exerted by desipramine on hERG, which ultimately should help to improve the cardiovascular safety of all TCAs.

EXPERIMENTAL PROCEDURES

Cell Culture—Human embryonic kidney (HEK) 293 cells stably expressing hERG WT, hERG WT HA_{ex}, bEAG, or hKv1.5 WT HA_{ex} (HA_{ex} indicates an extracellular hemagglutinin tag introduced in the S1-S2 linker (29)) were maintained at 37 °C, 5% CO_2 in DMEM supplemented with 10% fetal bovine serum, L-glutamine, penicillin/streptomycin (complete DMEM), and G418.

Neonatal rat ventricular myocytes (NRVMs) were isolated from dissected hearts of 1–2-day-old rat pups. All procedures conformed to institutional guidelines for the care and use of animals in research. Briefly, hearts were minced in HBSS, and tissue fragments were digested overnight with trypsin at 4 °C. In a second step, trypsinized tissue fragments were treated repeatedly for short periods of time with collagenase at 37 °C followed by trituration. Dissociated cells were filtered, collected via centrifugation, and pre-plated for 2 h at 37 °C in DMEM supplemented with 5% fetal bovine serum (FBS) and penicillin/streptomycin to remove fibroblasts. Supernatants were collected from "pre-plating" dishes, and NRVMs were replated in DMEM, 5% FBS, penicillin/streptomycin at a density of 4×10^6 cells/60-mm culture dish. NRVM cultures were maintained at 37 °C, 5% CO_2 with bromodeoxyuridine added to suppress fibroblast growth. For electrophysiological studies NRVMs were grown on collagen-coated glass coverslips. Experiments were typically performed 2–4 days after initial plating.

Drugs were added to cell cultures for either 6 h (short term) or 16–20 h (overnight) before Western blot analysis or current recordings. Stock solutions of desipramine, bafilomycin, astemizole, and dynasore were prepared in DMSO. Final DMSO concentrations in drug-containing solutions did not exceed 0.1%. Amitriptyline stock solutions were prepared in H_2O. Experiments with dynasore were performed in serum-free DMEM because dynasore binds to serum proteins and loses its activity (30).

Cellular Electrophysiology—HEK/hERG- and HEK/hKv1.5-expressing cells were recorded using patch pipettes filled with 100 mM potassium aspartate, 20 mM KCl, 2 mM $MgCl_2$, 1 mM $CaCl_2$, 10 mM EGTA, and 10 mM HEPES, (pH 7.2). The extracellular recording solution was 140 mM NaCl, 5 mM KCl, 1 mM $MgCl_2$, 1.8 mM $CaCl_2$, 10 mM HEPES, and 10 mM glucose (pH 7.4). In NRVMs, I_{Kr}/hERG currents were recorded in isotonic Cs^+ solutions (pipette: 135 mM CsCl, 1 mM $MgCl_2$, 10 mM EGTA, 10 mM HEPES (pH 7.2); extracellular recording solution: 135 mM CsCl, 1 mM $MgCl_2$, 10 mM HEPES, 10 mM glucose, 1 μM nisoldipine (pH 7.4) (31). PCLAMP software and an Axon 200B patch clamp amplifier (Molecular Devices, Sunnyvale, CA) were used for the generation of voltage clamp protocols and data acquisition. To analyze current densities, membrane capacitance was measured using the analog compensation circuit of the patch clamp amplifier. All current recordings were performed at room temperature (20–22 °C).

Western Blot Analysis—A previously described polyclonal anti-hERG antibody, rabbit hERG 519, was used to analyze hERG expression in HEK cells (29). In NRVMs I_{Kr}/hERG expression was analyzed using a polyclonal anti-hERG-GST antibody from Alomone Labs, Jerusalem, Israel. Briefly, HEK/hERG cells or NRVMs were solubilized for 1 h at 4 °C in lysis buffer containing 150 mM NaCl, 1 mM EDTA, 50 mM Tris, pH 7.5, 1% Triton X-100, and protease inhibitors (Complete, Roche Diagnostics). Protein concentrations were determined by the BCA method (Pierce). Proteins were separated on SDS-polyacrylamide gels, transferred to polyvinylidene difluoride membranes, and developed using the appropriate anti-hERG antibody followed by horseradish peroxidase-conjugated secondary antibody and ECL Plus (GE Healthcare). For quantitative analysis, signals were captured directly on an Eastman Kodak Co. Imager R4000 (Carestream Health).

hERG Internalization and Recycling Assays—Cleavable EZ-Link Sulfo-NHS-SS-Biotin (0.25 mg/ml; Pierce) was used to biotinylate cell surface proteins expressed in HEK/hERG cells for 30 min at 4 °C in PBS. The biotinylation reaction was quenched with 10 mM glycine. To measure hERG internalization, cells were incubated for the designated times ranging from 5 to 60 min in complete DMEM in the absence or presence of desipramine to allow for internalization of biotinylated cell surface proteins. At the end of each internalization period, cells were treated with the membrane-impermeable reducing agent MESNA (sodium 2-mercaptoethane-sulfonate, 50 mM in PBS) for 20 min at 4 °C to strip biotin labels from proteins remaining at the cell surface. Detergent-soluble cell lysates were prepared from MESNA-treated cells, and internalized biotinylated proteins were isolated using streptavidin-agarose (Thermo Scientific). Biotinylated proteins were released from streptavidin-agarose by boiling in Laemmli sample buffer, resolved on SDS-PAGE, and blotted with anti-hERG antibody. Non-reduced and reduced samples processed before internalization were used to determine the total amount of cell surface hERG present as well as any background remaining upon MESNA treatment.

To determine hERG recycling, HEK/hERG surface proteins were biotinylated as described above. Cells were then incubated in complete DMEM at 37 °C for 30 min to allow for internalization of biotinylated cell surface proteins. Next, cells were treated with MESNA to remove all biotin labels remaining at the cell surface. Then, cells were washed quickly with prewarmed complete DMEM to remove MESNA and incubated with complete DMEM at 37 °C for the designated times to allow for recycling of initially internalized biotinylated proteins back to the cell surface. Experiments were performed in the absence and presence of desipramine. At the end of each recycling period, biotinylated proteins were stripped again with MESNA. Cells were washed, lysed, and processed for hERG protein expression as described above. Note that hERG protein resolved on Western blots has been protected from MESNA. Consequently, the recycled fraction of hERG protein was determined by the difference between initially internalized hERG ($t = 0$) and hERG protein protected from MESNA at the end of recycling periods.

hERG Ubiquitination—In ubiquitination studies stable HEK/hERG WT cells were transiently transfected with either HA-ubiquitin or His_6-ubiquitin cDNA using FuGENE (Roche Diagnostics). Cells were harvested 2 days after transfection. In experiments with desipramine cells were treated on the second day after transfection for either 1–6 h or overnight. Whole cell lysates were immunoprecipitated with anti-hERG antibody. Duplicate samples of immunoprecipitates were analyzed on Western blots using either antibody to hERG or to the HA epitope fused to ubiquitin. Lysates from HEK/hERG cells transfected with His_6-ubiquitin were used as negative control.

Pulse-Chase and hERG-Chaperone Interaction Studies—Pulse-chase and hERG-chaperone interaction experiments were performed as described (29). Briefly, HEK/hERG WT cells were starved for 30 min and pulse-labeled for 60 min in 100–150 μCi/ml [^{35}S]methionine/cysteine-containing medium. Cells were harvested immediately after labeling or after different chase periods in label-free medium. Desipramine was added either for 24 h before labeling or during chase periods. Cells were lysed in a 0.1% Nonidet P-40 buffer in the presence of protease inhibitor. Immunoprecipitations with anti-hERG antibody (Alomone) were incubated overnight at 4 °C and collected with Protein G Dynabeads (Dynal, Lake Success, NY). Immunoprecipitated radiolabeled proteins were eluted from beads via boiling, separated by SDS-PAGE, and analyzed with a STORM PhosphorImager (GE Healthcare). In pulse-chase experiments image densities of fully glycosylated, and core-glycosylated hERGs were normalized to the signal of freshly synthesized, core-glycosylated hERG protein isolated immediately after radiolabeling at $t = 0$.

To study hERG-Hsp/c70 interactions, HEK/hERG WT cells were labeled and chased in the absence or presence of desipramine as described above. Immunoprecipitations reactions were performed either with anti-hERG or anti-Hsp/c70 antibody (Santa Cruz). Eluted samples were separated by SDS-PAGE and analyzed with a STORM PhosphorImager (29). In some experiments hERG-Hsp90 interactions were studied after treatment of labeled HEK/hERG cells with the chemical cross-linker dithiobis(succinimidyl propionate) (Pierce). Cross-linking was quenched by the addition of glycine and resolved by boiling in β-mercaptoethanol/SDS sample buffer to release proteins immunoprecipitated with Hsp90 antibody (Santa Cruz).

To quantify hERG-chaperone interactions at specific time points, image densities of core-glycosylated (cg) and fully glycosylated (fg) hERG protein bands were determined on autoradiograms after immunoprecipitation with anti-hERG and anti-Hsp/c70 antibodies. Image densities corresponding to cg- and fg-hERG found in immunoprecipitations were normalized to image densities of cg-hERG isolated immediately after labeling to assess time-dependent changes of cg-hERG and fg-hERG synthesis in the presence or absence of desipramine as well as changes in hERG-Hsp/c70 interactions as a function of drug exposure.

Immunocytochemistry—HEK-hERG cells were grown overnight on poly-lysine-coated glass coverslips under control conditions or in the presence of 30 μM desipramine. After incubation, cells were washed with PBS and fixed in ice-cold 4% formaldehyde, PBS for 30 min. After fixation, cells were washed, permeabilized with 0.1% Triton X-100, and blocked in 5% goat serum, PBS for 30–60 min at room temperature. For double labeling, permeabilized cells were incubated overnight at 4 °C with rabbit anti-hERG GST antibody (1:100; Alomone Labs) and mouse anti-KDEL antibody (1:100; Stressgen Biotechnology, Collegeville, PA). The tetrapeptide KDEL, located at the carboxyl-terminal sequences of luminal ER proteins, is a common motif expressed in the ER that is well suited as a compartment marker. Primary antibodies were washed off using PBS, and cells were re-blocked in 5% goat serum (30 min) and incubated for 2 h at room temperature with secondary anti-rabbit FITC (1:100; The Jackson Laboratory, Bar Harbor, ME) and anti-mouse Rhodamine RedX antibody (1:100, The Jackson Laboratory). Coverslips were mounted with Vectashield and examined using a Leica TCS SP2 laser scanning confocal microscope (Leica).

Detection of hERG Internalization by Immunocytochemistry—Stably transfected HEK/hERG WT HA_{ex} cells were grown on glass coverslips coated with the ECL attachment matrix (Upstate Biotechnology/Millipore). To label cell surface hERG-HA_{ex}, cells were treated for 30 min at room temperature with a 1:100 dilution of rat monoclonal anti-HA antibody (Roche Diagnostics, high affinity clone) in DMEM. After removal of unbound antibody, cells were incubated at 37 °C, 5% CO_2 in complete DMEM medium for various amounts of time in the absence or presence of desipramine to allow for channel internalization. After incubation at 37 °C cells were washed, fixed with 4% paraformaldehyde for 15 min, permeabilized, blocked with 5% donkey serum for 30 min, and stained with Alexa Fluor 488-conjugated donkey anti-rat secondary antibody for 1 h in blocking medium. Subsequently, stained coverslips were mounted with Vectashield and inspected using a Leica TCS-SP2 microscope in the fluorescent and brightfield/differential interference contrast mode to study changes in the subcellular localization of hERG as a function of incubation time.

To simultaneously detect cell surface and internalized hERG HA_{ex}, cells were labeled with rat anti-HA antibody as described above and incubated for various time periods at 37 °C, 5% CO_2 to allow for channel internalization. Cells were then washed,

fixed with paraformaldehyde, blocked, and labeled with anti-rat Alexa Fluor 488-conjugated secondary antibody before permeabilization to stain the cell surface pool of hERG-HA_{ex}. Subsequently, cells were permeabilized for 5 min at RT with 0.1% Tween 20. After permeabilization, cells were re-blocked with donkey serum in PBS-0.1% Tween 20 for 30 min at RT and stained with donkey anti-rat Red X-conjugated secondary antibody to label the pool of internalized hERG channels.

To co-stain cells for hERG HA_{ex} and the early endosomal marker EEA1, cells were first labeled with rat anti-HA antibody as described and incubated for various times at 37 °C, 5% CO in complete DMEM medium (±desipramine). Next, cells were fixed, permeabilized with 0.1% Tween 20, PBS, blocked with 5% donkey serum, and labeled with mouse anti-EEA1 antibody (BD Biosciences, 1:100) for 1 h at RT. After washes with PBS, cells were stained with a combination of anti-rat Alexa Fluor 488- and anti-mouse Red-X-conjugated secondary antibodies to co-localize hERG and EEA1 proteins.

To co-localize hERG with LAMP1-EGFP, which is used as a lysosomal marker (32), LAMP1-EGFP was transfected transiently into HEK/hERG HA_{ex} cells using FuGENE (Roche Diagnostics). Twenty-four hours later, surface hERG was labeled using rat anti-HA antibody, and cells were incubated for various times in complete DMEM at 37 °C, 5% CO_2 (±desipramine). After fixation and permeabilization, cells were stained with anti-rat Red X-conjugated secondary antibody for 1 h at RT to visualize hERG in addition to LAMP1-EGFP.

Data Analysis—Data are expressed as the mean ± S.E. of *n* experiments or cells studied. Differences between means were tested using either a two-tailed Student's *t* test or single factor analysis of variance followed by a two-tailed Dunnett's test to determine whether multiple treatment groups were significantly different from control. *p* values <0.05 were considered statistically significant.

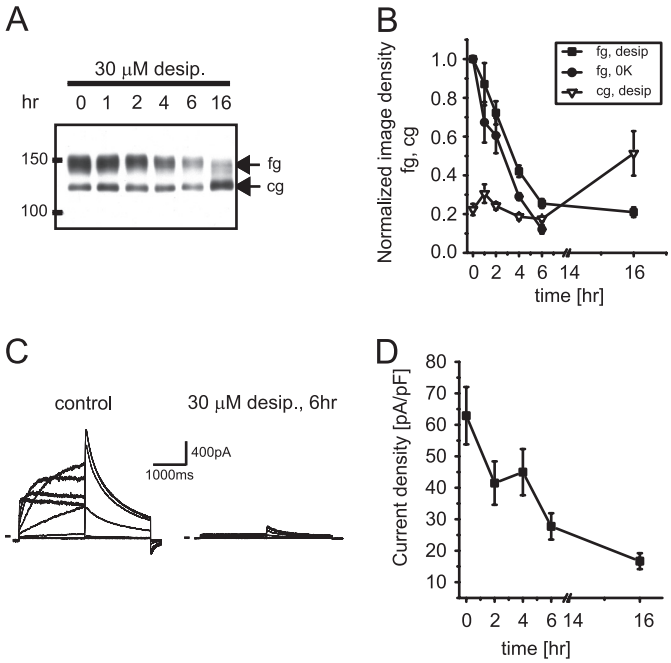

FIGURE 1. **Desipramine reduces hERG surface expression on short term exposure.** *A*, Western blot shows time-dependent effects of incubation with 30 μM desipramine (*desip.*) on hERG protein stably expressed in HEK293 cells. Equal amounts of protein were loaded; *fg* indicates glycosylated, 150-kDa cell surface form of hERG; *cg* indicates core-glycosylated, 135-kDa ER-resident form of hERG. *B*, quantitative analysis of time-dependent changes in fg- and cg-hERG levels after exposure to 30 μM desipramine is shown. Effects of 0 K^+ on fg-hERG are included for comparison. Image densities on Western blots were normalized to fg-hERG levels measured at $t = 0$. Note that cg-hERG is increased at $t = 16$ h ($n = 3–4$). *C*, shown are representative hERG current families recorded under control conditions or after a 6-h exposure to 30 μM desipramine. Currents were elicited using depolarizing voltage steps from −60 to +60 mV. Tail currents were recorded on return to −50 mV. Holding potential was −80 mV. *D*, time-dependent reduction of hERG tail current densities on exposure to 30 μM desipramine ($n = 6–17$) is shown. Data are given as the mean ± S.E.

RESULTS

Desipramine Reduces hERG Surface Expression—We have recently reported that desipramine reduces cell surface expression of hERG within 1–2 h (11), which is not easily reconciled with a half-life of 11 h for hERG channels at the cell surface under control conditions (29). To characterize desipramine effects on hERG surface expression in more detail, we exposed HEK/hERG cells for extended time periods of 1–16 h to 30 μM desipramine, a concentration selected to produce robust short term effects, thereby facilitating biochemical analysis. In a first series of experiments we studied time-dependent expression changes by Western blot (Fig. 1*A*). For comparison, we used HEK/hERG cells treated with $0[K^+]_{ex}$, because fast internalization and degradation of hERG channels via endocytotic pathways has been demonstrated under low K^+ conditions (33). We found that desipramine incubation reduced the fully glycosylated 155-kDa cell surface form of hERG (fg-hERG) within 6 h by 70–80% (Figs. 1, *A* and *B*). However, expression of the core-glycosylated 135-kDa ER resident form of hERG (cg-hERG) was not altered upon short -term incubation yet increased significantly on long term exposure to desipramine (16 h), suggesting that two independent pathways may regulate surface expression. The fast decrease in fg-hERG expression seen on Western blots was also mirrored in electrophysiological current recordings performed after desipramine had been washed out for at least 10 min. In these experiments hERG current density was reduced from 62.9 ± 9.1 ($n = 17$) to 27.7 ± 4.2 pA/pF ($n = 12$) within 6 h of exposure to 30 μM desipramine (Fig. 1, *C* and *D*). The observed current changes reflected predominantly altered surface expression with very little residual block present because wash-out of 30 μM desipramine was best described by a time constant of 53.3 s ($n = 4$). Together these experiments describe a fast, drug-induced change in hERG surface expression that mimics data acquired under low K^+ conditions (see Fig. 1*B*).

Analysis of Desipramine Effects in Neonatal Rat Ventricular Myocytes—In addition to our experiments in a heterologous expression system, we have also studied desipramine effects on native I_{Kr}/rERG channels expressed in cultured NRVMs. To assess desipramine effects on rERG protein, NRVMs were incubated with desipramine for either 6 h or overnight (17 h). On Western blots desipramine reduced the fully glycosylated cell surface form of rERG both on short (6 h) as well as on long term (17 h) drug exposure (Fig. 2*A*). In addition, we monitored whether the reduction of cell surface rERG was accompanied by a corresponding decrease in I_{Kr} current amplitudes. NRVM I_{Kr} currents were isolated in symmetrical Cs^+ solutions and elic-

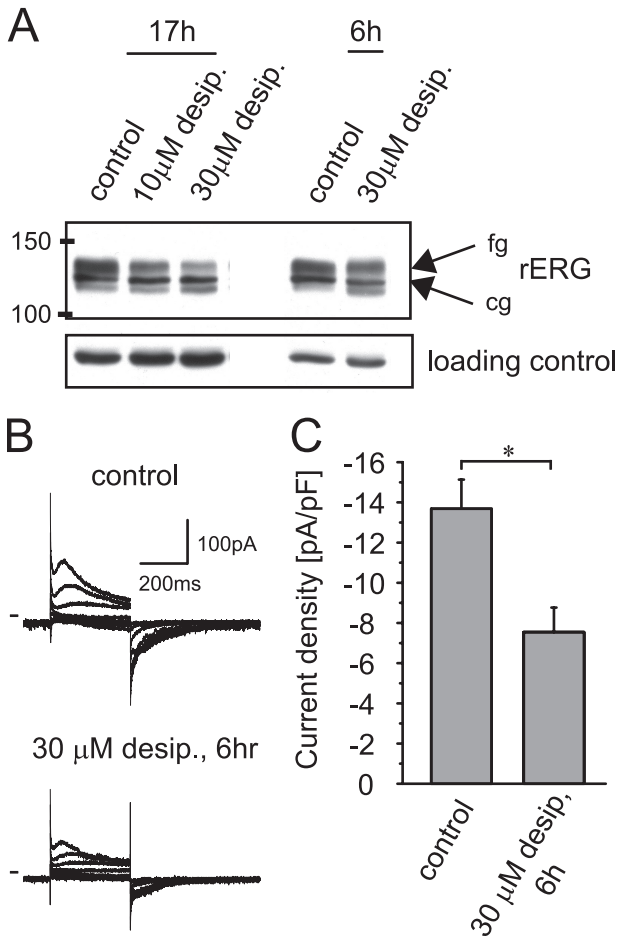

FIGURE 2. **Desipramine suppresses endogenous rERG/I_{Kr} currents in NRVM on short term incubation.** *A*, Western blot shows rERG under control conditions after overnight (17 h) exposure to either 10 or 30 μM desipramine and after a 6-h exposure to 30 μM desipramine. *B*, rERG currents were recorded under control conditions or after a 6-h exposure to 30 μM desipramine. Currents were elicited in symmetric Cs^+ solutions using depolarizing test pulses from −60 to + 60 mV. Holding potential was −80 mV. *C*, quantitative analysis of maximal rERG tail current densities recorded on return to −80mV under control conditions or after a 6-h exposure to 30 μM desipramine ($n = 6$) is shown. Data are given as the mean ± S.E. Note that current densities were significantly different at $p < 0.05$ level.

ited using 350-ms depolarizing test pulses from a holding potential of −80 mV (Fig. 2*B*). Maximal I_{Kr} tail current amplitudes measured on return to −80 mV were reduced from −14 pA/pF under control conditions to −7pA/pF ($n = 6$) after a 6-h incubation with 30 μM desipramine, resembling our findings in HEK/hERG cells (Fig. 2*C*).

Drug-induced hERG Internalization—To explore whether desipramine may alter hERG surface expression along endocytic pathways, we used a stable cell line expressing hERG WT with an HA epitope tag inserted in the extracellular S1-S2 domain (hERG WT HA_{ex} (29)) to directly visualize channel internalization. In these cells hERG-HA_{ex} was prelabeled at the cell surface with anti-HA antibody. Subsequently, cells were incubated at 37 °C for various time periods to allow for hERG internalization before fixation, permeabilization, and staining with Alexa Fluor 488-conjugated secondary antibody (Fig. 3). Alternatively, cell surface channels were detected with Alexa Fluor 488-conjugated secondary antibody in non-permeabilized cells, whereas internalized channels were detected with

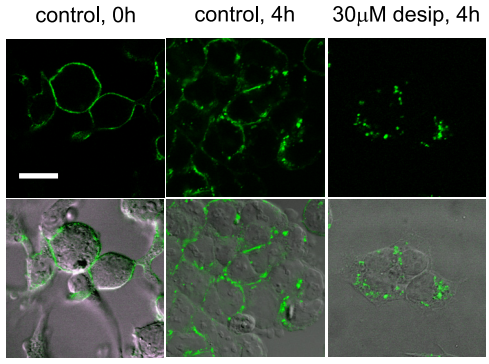

FIGURE 3. **Desipramine increases internalization of cell surface hERG channels.** Stably transfected hERG-HA_{ex} cells were prelabeled with anti-HA antibody and incubated for 4 h either under control conditions or in the presence of 30 μM desipramine before fixation, permeabilization, and staining with Alexa Fluor 488-conjugated secondary antibody. Shown are confocal fluorescence images (*top row*) together with corresponding brightfield images with overlaid fluorescence staining (*bottom row*). Note that desipramine leads to accumulation of cell surface hERG in large intracellular vesicles. *Scale bar*, 20 μm.

RedX-conjugated secondary antibody after permeabilization (supplemental Fig. 1). When cells were analyzed immediately after prelabeling of surface channels ($t = 0$), we detected uniform cell surface staining that was largely preserved after incubation at 37 °C under control conditions. This indicated that the majority of hERG channels remained at the cell surface. In marked contrast, incubation with desipramine initiated a fast, time-dependent internalization process that resulted in removal of most channels from the cell surface and accumulation in enlarged, intracellular vesicles (Fig. 3; supplemental Fig. 1).

Specificity of Desipramine Effects—Because desipramine is a cationic amphiphilic drug known to modify a wide range of physicochemical membrane properties as well as pH of acidic intracellular vesicles, it is possible that desipramine reduces surface expression of ion channels in a global, nonspecific manner. To the contrary, we have shown previously that cardiac action potentials were prolonged in the presence of desipramine due to a targeted suppression of I_{Kr}/hERG currents (11). To address specificity more directly, we studied heterologously expressed hKv1.5, another major cardiac potassium channel known to undergo fast endocytic recycling processes (34–36). We found that hKv1.5 currents were neither affected on short (3–6 h) nor on long term (overnight) exposure to desipramine (Fig. 4, *A*–*C*). Lack of effect was not explained by desipramine-induced inhibition of hKv1.5 internalization because immunocytochemical analysis showed no difference in hKv1.5 internalization in the absence or presence of desipramine (supplemental Fig. 2). To explore a channel that is more closely related to hERG with a high degree of sequence homology, we tested bEAG and found that current densities were not significantly altered upon short term as well as overnight exposure to 30 μM desipramine. We recorded 581 ± 82 pA/pF (at +40 mV; $n = 13$) under control conditions, 478 ± 99 pA/pF ($n = 15$) after 3 h of exposure to 30 μM desipramine, 628 ± 107 pA/pF ($n = 15$) after 6 h of drug exposure, and 483 ± 52 pA/pF ($n = 11$) after overnight drug exposure (supplemental Fig. 3).

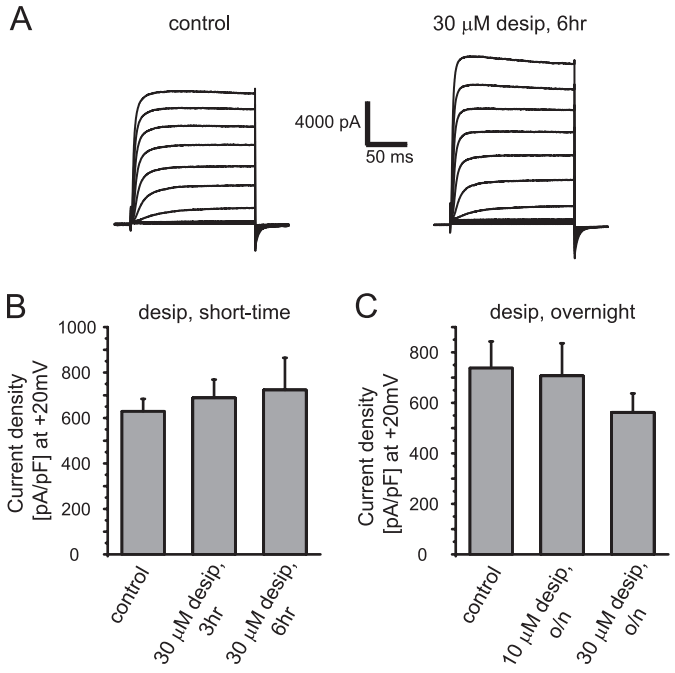

FIGURE 4. **Desipramine does not alter hKv1.5 expression.** *A*, representative hKv1.5 current families recorded under control conditions or after a 6-h exposure to 30 μM desipramine are shown. Currents were elicited using depolarizing voltage steps from −70 to +40 mV. Tail currents were recorded on return to −100 mV. Holding potential was −80 mV. *B*, quantitative analysis of hKv1.5 current densities measured under control conditions or after incubation with 30 μM desipramine for 3 or 6 h is shown. *C*, quantitative analysis of hKv1.5 current densities after overnight incubation with 10 or 30 μM desipramine is shown. Data are presented as the mean ± S.E.

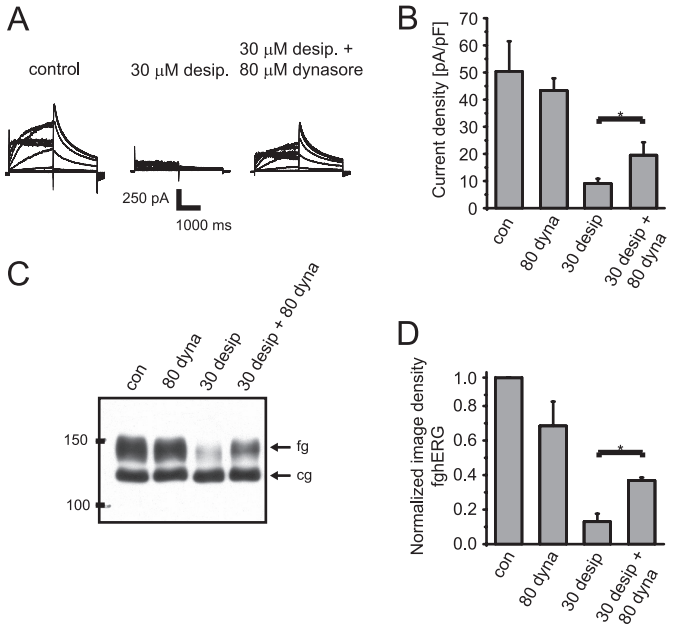

FIGURE 5. **Desipramine effects are attenuated in the presence of the dynamin inhibitor dynasore.** *A*, representative hERG current families recorded under control conditions after a 6-h exposure to 30 μM desipramine or after a 6-h exposure to a combination of 30 μM desipramine and 80 μM dynasore are shown. Voltage protocol was the same as in Fig. 1. *B*, quantitative analysis of hERG tail current densities was measured under control conditions, after exposure to 80 μM dynasore (*dyna*, 6 h), 30 μM desipramine (6 h), or a combination of 30 μM desipramine and 80 μM dynasore (6 h) ($n = 5–8$). *C*, Western blot shows the effects of incubation with 80 μM dynasore (6 h), 30 μM desipramine (6 h), or a combination of 30 μM desipramine and 80 μM dynasore (6 h) on hERG protein stably expressed in HEK293 cells. *fg* indicates the fully glycosylated, 150-kDa cell surface form of hERG; *cg* indicates the core-glycosylated, 135-kDa ER-resident form of hERG. *con*, control. *D*, quantitative analysis of fg-hERG image densities after incubation with 80 μM dynasore (6 h), 30 μM desipramine (6 h), or a combination of 30 μM desipramine and 80 μM dynasore (6 h) is shown. Image densities were normalized to fg-hERG levels measured under control conditions ($n = 3–4$). Experiments with dynasore were performed in media that lack both albumin and serum to preserve its activity. Data are presented as the mean ± S.E. *Asterisks* indicate significant differences at $p < 0.05$ level.

Desipramine-induced hERG Channel Internalization—One explanation for the desipramine-induced decrease in hERG surface expression may be increased channel internalization. To disrupt internalization processes at the cell surface, we inhibited the GTPase dynamin, which is essential for pinching off transport vesicles from the plasma membrane along most endocytotic pathways using dynasore. Dynasore is a specific cell-permeable inhibitor of dynamin-dependent internalization pathways, *e.g.* in neurons or HL-1 cardiomyocytes. It is most often used at a concentration of 80 μM, which is thought to block about 90% of all endocytotic events (30). Although short term incubation with 80 μM dynasore did not significantly alter hERG surface expression under control conditions (Figs. 5, *C* and *D*), dynasore partially rescued hERG surface expression and function in the presence of desipramine (Fig. 5, *A–D*).

Because our experiments with dynasore indicated that desipramine increased hERG internalization, we used a biotin protection assay to directly measure channel internalization during desipramine exposure (37). In these experiments a cleavable, membrane-impermeable biotin label was coupled to cell surface hERG before incubation of HEK/hERG cells at 37 °C. Biotin labels that remained at the cell surface at the end of incubation periods were stripped with MESNA, a membrane-impermeable reducing agent. Subsequently, HEK/hERG cells were lysed, and internalized biotin-labeled hERG was isolated on streptavidin-based affinity columns for Western analysis (Fig. 6*A*). We determined that under control conditions 21.2% of initially labeled cell surface hERG was internalized within 60 min (Fig. 6*B*). Surprisingly, in the presence of desipramine only 9.7% of cell surface hERG was internalized at 60 min (Fig. 6*B*). We also measured channel recycling using a variant of the above described biotin protection assay (see "Experimental Procedures") and found that 80% of internalized channels was returned to the cell surface within 2–3 min under control or desipramine-treated conditions (Fig. 6*C*).

Desipramine-induced Ubiquitination and Degradation of hERG—Because desipramine-induced reduction in hERG surface expression appeared to be due to neither enhanced internalization nor reduced recycling, we asked whether desipramine might cause hERG ubiquitination and degradation upon short term drug exposure. To test with high fidelity for time-dependent changes in channel ubiquitination, we expressed hERG WT together with HA- or His_6-tagged ubiquitin. Ubiquitin-transfected HEK/hERG cells were either cultured under control conditions or exposed to 30 μM desipramine for 1, 3, or 6 h. After immunoprecipitation with anti-hERG antibody, immunoprecipitates were blotted with either anti-hERG or anti-HA antibody to detect multi-ubiquitinated hERG proteins. On Western blots we detected a fast, time-dependent increase in hERG ubiquitination that mirrored the reduction of fully glycosylated cell surface hERG seen in the presence of desipra-

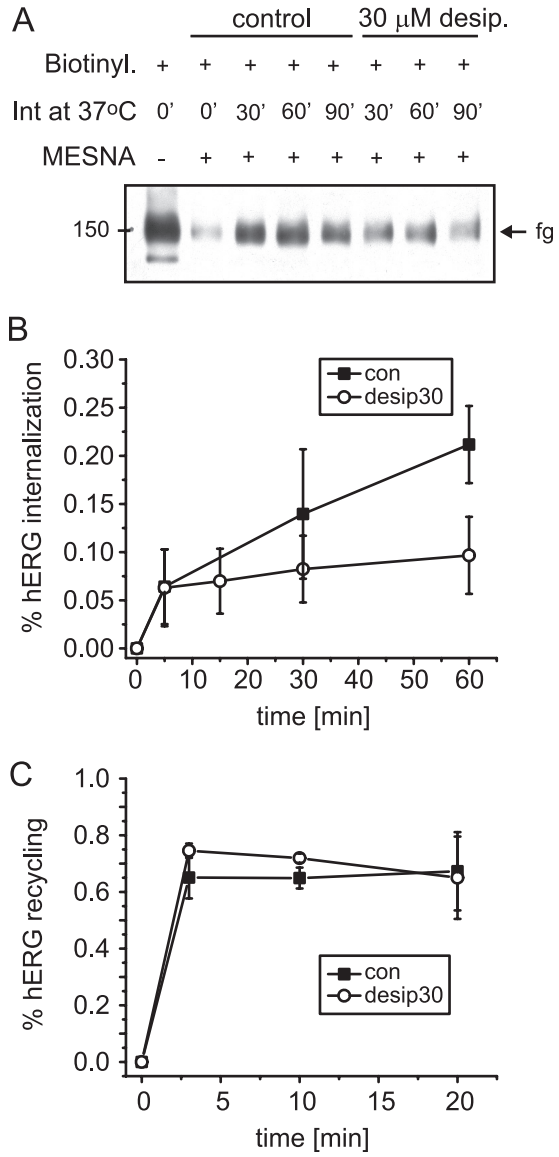

FIGURE 6. **Endocytic recycling of hERG in stably transfected HEK cells.** *A*, shown is a representative Western blot obtained from a biotin protection assay used to measure hERG internalization under control conditions or in the presence of 30 μM desipramine. From *left* to *right*, total cell surface hERG biotinylated under control conditions; cell surface hERG isolated after stripping of biotin labels from cell surface with the reducing agent MESNA; amount of biotinylated cell surface hERG internalized during incubations of 30, 60, and 90 min at 37 °C under control conditions; amount of biotinylated cell surface hERG internalized during incubations of 30, 60, and 90 min at 37 °C in the presence of 30 μM desipramine. *B*, time-dependent internalization of cell surface hERG measured under control (*con*) conditions or in the presence of 30 μM desipramine (n = 3–4) is shown. Note that incubation with desipramine appears to reduce hERG internalization. *C*, time-dependent recycling of internalized hERG back to the cell surface measured under control conditions or in the presence of 30 μM desipramine (n = 3) is shown. Data are presented as the mean ± S.E.

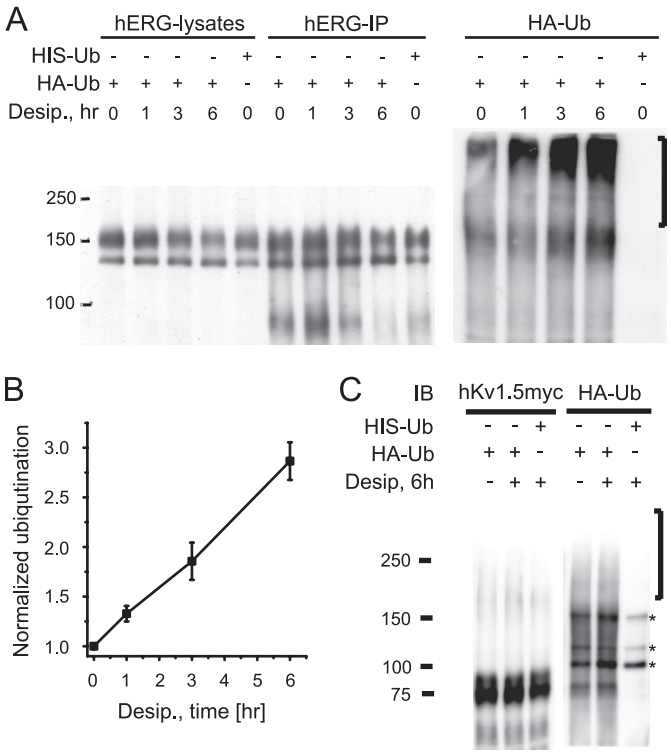

FIGURE 7. **Desipramine increases hERG ubiquitination.** *A*, shown is a Western blot analysis of HEK/hERG cells transiently transfected with HA-tagged ubiquitin and treated for 1, 3, or 6 h with 30 μM desipramine. Transfection with His_6-ubiquitin was used as negative control. Whole cell lysates, shown in the *right part of the panel*, were immunoprecipitated with anti-hERG antibody, resolved by SDS-PAGE, and immunoblotted using either anti-hERG antibody (*hERG-IP*) or an antibody recognizing the HA epitope fused to ubiquitin (*HA-Ub*). Immunoblotting with anti-HA antibody identifies high molecular weight forms of ubiquitinated hERG that are increased on prolonged exposure to 30 μM desipramine. *B*, shown is a quantitative analysis of hERG ubiquitination as a function of desipramine exposure (n = 3). Image densities corresponding to ubiquitinated hERG were measured in a region of HA-Ub Western blots indicated by a *black bar to the right of panel A*. Image densities were normalized to Ub-hERG levels measured under control conditions. *C*, shown is a Western analysis (*IB*, immunoblot) of HEK cells co-transfected with h-Kv1.5myc and either HA- or HIS_6-tagged ubiquitin. Shown are immunoprecipitations of hKv1.5 protein with anti-myc antibody under control conditions or after treatment with 30 μM desipramine for 6 h. Samples were analyzed using anti-HA antibody to identify putative high molecular weight forms of ubiquitinated hKv1.5. Transfection with His_6-ubiquitin was used as a negative control. *Asterisks to the right of the panel* indicate non-specifically stained protein bands. Note that desipramine does not increase HA-Ub staining in high molecular weight region (*black bar to the right of the panel*) where multi-ubiquitinated hKv1.5 would be expected.

mine (Fig. 7*A*). In fact, the dark smear extending from 150 kDa to the top of the SDS-PAGE (Fig. 7*A*, *right panel*, *black bar*), reflecting channel ubiquitination, increased linearly with longer drug exposure times and tripled its density within 6 h (Fig. 7*B*). In marked contrast, Kv1.5 ubiquitination was not significantly affected by desipramine (Fig. 7*C*), in agreement with our observation that Kv1.5 surface expression was not altered. Importantly, Kv1.5 was strongly ubiquitinated in the presence of 100 nM Velcade/bortezomib, a potent proteasomal inhibitor (supplemental Fig. 4).

Because desipramine increased hERG ubiquitination, we next asked whether the channel was subsequently degraded along proteasomal or lysosomal pathways. Hence, HEK/hERG cells were incubated for 6 h with 30 μM desipramine and either 100 nM Velcade/bortezomib, a proteasomal inhibitor, or 10 nM bafilomycin, a lysosomal inhibitor. As a negative control we employed the pharmacological chaperone astemizole, which has been used to restore conformational trafficking defects of hERG yet is not known to interfere with cellular degradation pathways (38). We found that expression of fully glycosylated hERG was partially restored in the presence of desipramine by the lysosomal inhibitor bafilomycin as judged from Western blots, whereas neither Velcade/bortezomib nor astemizole

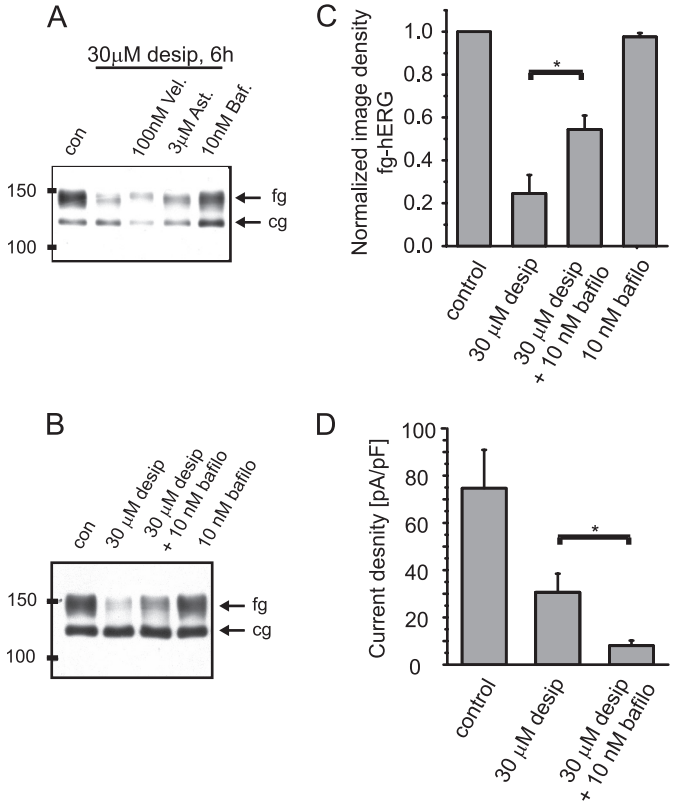

FIGURE 8. **Desipramine effects are rescued by the lysosomal inhibitor bafilomycin.** *A*, Western blot shows hERG protein under control (*con*) conditions after a 6-h exposure to 30 μM desipramine and after a 6-h co-incubation of 30 μM desipramine with either 100 nM Velcade (*Vel*)/bortezomib or 3 μM astemizole (*Ast*) or 10 nM bafilomycin (*Baf*). *B*, Western blot showing the effects of 30 μM desipramine (6 h) of co-incubation of desipramine with 10 nM bafilomycin (*bafilo*, 6 h) and of 10 nM bafilomycin alone (6 h) on hERG protein stably expressed in HEK cells. *fg* indicates the fully glycosylated, 150-kDa cell surface form of hERG; *cg*, indicates the core-glycosylated, 135-kDa ER-resident form of hERG. *C*, shown is a quantitative analysis of fg-hERG image densities after incubation with 30 μM desipramine (6 h), a combination of 30 μM desipramine and 10 nM bafilomycin (6 h), and with 10 nM bafilomycin alone. Image densities were normalized to fg-hERG levels measured under control conditions ($n = 3–6$). *D*, shown is quantitative analysis of hERG tail current densities measured under control conditions on exposure to 30 μM desipramine (6 h) and on exposure to a combination of 30 μM desipramine and 10 nM bafilomycin (6 h; $n = 5–7$). Note that bafilomycin does not rescue hERG current levels in the presence of desipramine. Data are given as the mean ± S.E. *Asterisks* indicate significant differences at $p < 0.05$ level.

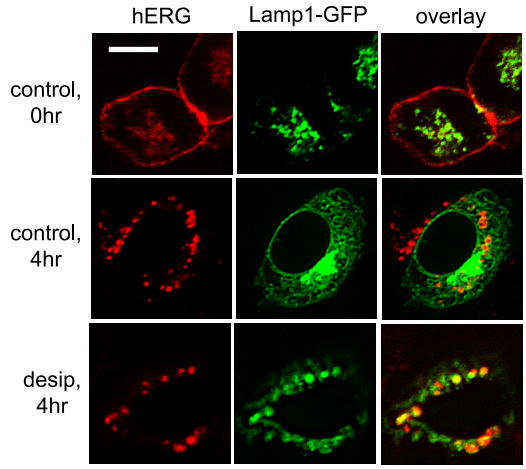

FIGURE 9. **Desipramine increases co-localization of hERG channels with Lamp1.** HEK/hERG-HA$_{ex}$ cells transiently transfected with Lamp1-GFP, a lysosomal marker protein, were prelabeled with anti-HA antibody and incubated for 4 h either under control conditions or in the presence of 30 μM desipramine before fixation, permeabilization, and staining with RedX-conjugated secondary antibody. Shown are representative confocal images. *Scale bar*, 20 μm.

were effective (Fig. 8*A*). Interestingly, rescue of fully glycosylated hERG expression by bafilomycin was not accompanied by an increase in functional channels at the cell surface, as determined by electrophysiological experiments (Fig. 8, *B–D*). This implies that rescued channels are retained in an intracellular compartment and are not restored to the cell surface membrane after co-incubation with bafilomycin. To identify intracellular compartments where hERG channels may traverse in the presence of desipramine, we studied co-localization of endocytosed hERG with either EEA1, a marker for early endosomes, or Lamp1, a marker for lysosomes. We detected co-localization of hERG with EAA1 antigen in the absence and presence of desipramine (supplemental Fig. 5). In marked contrast, co-localization with EGFP-tagged Lamp1 was increased in the presence of desipramine as expected from experiments with bafilomycin (Fig. 9). Taken together, our data suggest that short term exposure to desipramine induces rapid ubiquitination of recycling hERG channels and movement into lysosomes for degradation.

Desipramine Inhibits Forward Trafficking—Although alterations in endocytosis may explain the reduction of fully glycosylated cell surface hERG seen on short term desipramine exposure, this mechanism does not explain why the core-glycosylated ER resident form of hERG was increased with long term drug exposure (see Fig. 1*B*). Because it has been shown that accumulation of core-glycosylated hERG is indicative of impaired forward trafficking, we performed pulse-chase experiments to directly monitor hERG maturation in the presence and absence of desipramine. In these experiments complex glycosylation of hERG represents a well defined marker for ER export. Accordingly, we analyzed hERG maturation in HEK/hERG cells cultured under control conditions or incubated overnight with 30 μM desipramine. We found that hERG maturation from the initially synthesized 135-kDa ER resident form to the fully glycosylated 155-kDa form was largely blocked by long term incubation with desipramine, whereas synthesis and turnover of ER resident cg-hERG was not affected (Fig. 10, *A* and *B*). To narrow the time course of this effect, newly synthesized hERG was labeled with ^{35}S followed by chase with unlabeled media in the presence or absence of desipramine for up to 3 h (Fig. 10*C*). These experiments revealed that desipramine inhibited forward trafficking within 1 h. To test for ER retention as a consequence of long term drug exposure, we co-labeled HEK/hERG cells with anti-hERG and anti-KDEL (a well established ER marker) antibodies under control conditions and after desipramine exposure for 6 h or overnight (Fig. 11). Under control conditions hERG was stained at the cell surface, in a vesicular intracellular compartment, and in the ER. After 6 h, desipramine exposure cell surface staining was no longer detectable, whereas hERG was still present both in the vesicular and ER compartments. Finally, after overnight drug exposure, hERG staining was restricted to the ER, where it accumulated in bright foci, suggesting that hERG channels aggregated and failed to be exported from the ER.

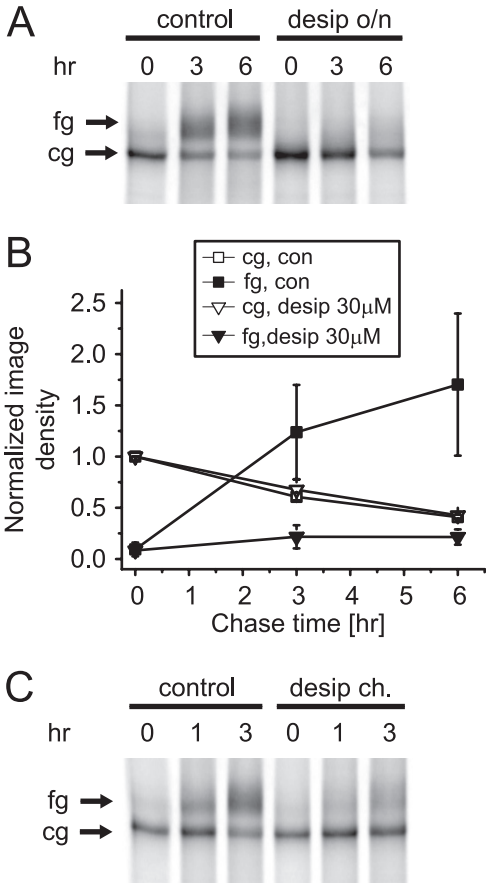

FIGURE 10. **Desipramine inhibits hERG forward trafficking.** *A*, shown is a pulse-chase analysis of hERG maturation in ^{35}S-labeled HEK/hERG cells under control conditions or after overnight (*o/n*) incubation with 30 μM desipramine. Radiolabeled hERG was isolated by immunoprecipitation after the chase periods indicated. *Arrows* indicate the position of fully fg and cg forms of hERG. *B*, quantitative analysis of time-dependent changes of fg- and cg-hERG densities measured under control conditions or after overnight incubation with 30 μM desipramine (n = 3). *C*, shown is a pulse-chase experiment performed with 30 μM desipramine present during the chase (*ch.*) period but not during synthesis of hERG protein. Note the fast suppression of hERG maturation by desipramine. Data are given as the mean ± S.E.

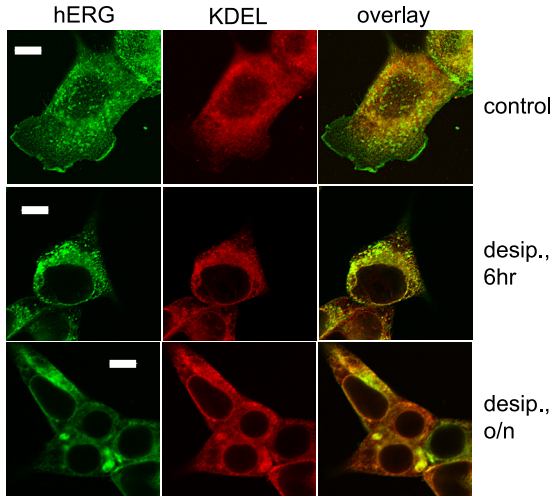

FIGURE 11. **Subcellular immunolocalization of hERG protein under control conditions, after 6 h of exposure to 30 μM desipramine (6 h), and after overnight exposure to 30 μM desipramine (*o/n*).** HEK/hERG cells were fixed, permeabilized, and double-labeled with anti-hERG and anti-KDEL antibody, which was used as marker of the ER. In untreated control cell hERG was localized to the cell surface, an intracellular vesicular fraction, and the ER. In cells treated with desipramine for 6 h, hERG staining was no longer detected at the cell surface. After overnight treatment with desipramine hERG staining was restricted to the ER, where it accumulated in brightly stained foci. *Scale bar*, 20 μm.

Does Desipramine Alter hERG-Chaperone Interactions?—Possible explanations for desipramine-induced ER retention may be 1) inhibition of chaperone association in the hERG export pathway as described for geldanamycin (29) or 2) drug-induced channel misfolding leading to prolonged hERG-chaperone interactions and ER retention as described for trafficking deficient LQT2 missense mutations (29). Consequently, we studied the interaction of hERG WT with the major cytosolic chaperones Hsp/c70 (Fig. 12, *A–C*) immediately after synthesis or after a chase period of 6 h in HEK/hERG cells cultured under control conditions or, overnight incubation with desipramine. Importantly, there was no difference in the formation or stability of hERG-Hsp/c70 complexes in desipramine *versus* control conditions (Figs. 12, *A* and *C*). In addition, we assessed the stability of hERG-Hsp90 complexes and found that those complexes were also not disrupted by desipramine (supplemental Fig. 6). Thus, desipramine-induced inhibition of hERG forward trafficking is unlikely to be mediated via impaired channel association with the cytosolic chaperones Hsp70/90. In contrast, we were able to show that hERG ubiquitination levels were increased after overnight incubation with desipramine (Fig. 12*D*). Therefore, it is possible that channel ubiquitination as a consequence of aggregation may also account for the reduction of ER export seen upon long term desipramine exposure.

Is Increased Channel Ubiquitination a Class Effect of TCAs?—To gain first insight we studied another TCA family member, amitriptyline, that in contrast to desipramine is a tertiary amine. Although it has been reported that acute block of hERG by amitriptyline is half-maximal with concentrations of 1–3 μM (hERGAPDbase), it has not been explored whether prolonged drug exposure may also affect hERG surface expression. Therefore, we incubated HEK/hERG cells overnight with increasing concentrations of amitriptyline and found decreasing amounts of fully glucosylated mature hERG on Western blots (Fig. 13*A*). In parallel, hERG tail currents were reduced with an IC_{50} value of 21.2 ± 0.4 μM (n = 7–13; Fig. 13*B*). In addition, we analyzed short term effects of 30 μM amitriptyline (Fig. 13*C*). In these experiments we recorded 66.3 ± 7.5 pA/pF (n = 10) under control conditions, 52.0 ± 8.6 pA/pF (n = 9) after 3 h of exposure to 30 μM amitriptyline, and 33.3 ± 4.8 pA/pF after 6 h of drug exposure (n = 10; Fig. 13*D*), which was comparable with current suppression seen on short term incubation with desipramine (Fig. 13*E*). Having established amitriptyline effects on hERG surface expression, we tested whether reductions in surface expression were coupled to increased channel ubiquitination as shown for desipramine. To this end we cultured HEK/hERG cells transfected with HA-ubiquitin under control conditions or in the presence of 30 μM amitriptyline for 3 and 6 h or overnight. After immunoprecipitations with anti-hERG antibody, we detected on Western blots an increase in hERG ubiquitination after short term as well as overnight incubation with amitriptyline (Fig. 13*F*). Likewise, hERG ubiquitination was increased on incubation with tetracyclic amoxapine, whose

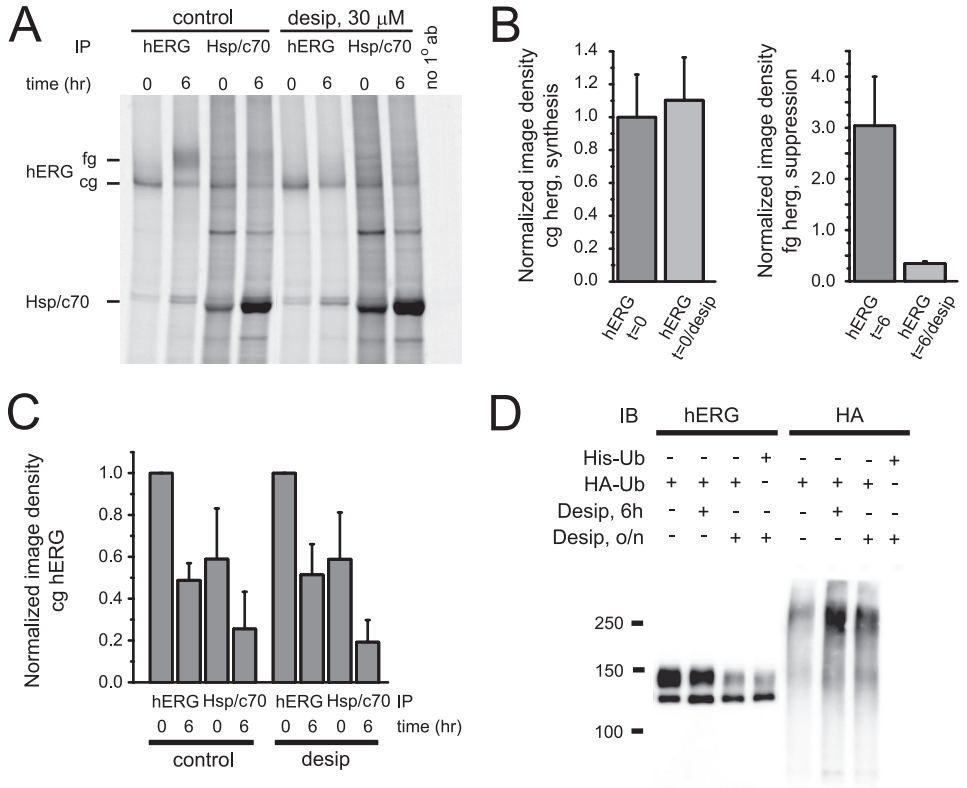

FIGURE 12. **Desipramine does not interfere with Hsp70 function.** *A*, shown is a pulse-chase experiment performed in the absence and presence of 30 μM desipramine. Radiolabeled hERG protein was isolated using immunoprecipitation (*IP*) with anti-hERG or anti-Hsp/c70 antibody after chase periods indicated. To the *left of the panel* the positions of fg/cg hERG and of Hsp/c70 on the autoradiogram are indicated. The *right-most lane* represents a negative control with no primary antibody added. *B*, *left panel*, quantitative analysis of hERG synthesis in the absence and presence of 30 μM desipramine ($n = 3$) is shown. *Right panel*, shown is a quantitative analysis of fg-hERG suppression after a 6-h exposure to 30 μM desipramine ($n = 3$). *C*, quantitative analysis of time-dependent formation of hERG-Hsp/c70 complexes in the absence and presence of desipramine ($n = 3–4$) is shown. Note that Hsp/c70 association is not different between control and desipramine-treated cells. *D*, shown is Western blot (*IB*) analysis of HEK/hERG cells transiently transfected with HA-tagged ubiquitin and treated for 6 h or overnight (*o/n*) with 30 μM desipramine. Transfection with HIS_6-ubiquitin was used as negative control. Whole cell lysates were immunoprecipitated with anti-hERG antibody, resolved by SDS-PAGE, and analyzed using either anti-hERG antibody or an antibody recognizing the HA epitope fused to ubiquitin. Immunoblotting with anti-HA antibody identifies high molecular weight forms of ubiquitinated hERG that are increased after either 6 h or overnight exposure to 30 μM desipramine.

multiple effects on hERG we have characterized previously (10) (supplemental Fig. 7).

DISCUSSION

We have expanded on our previous analysis of the tricyclic antidepressant and hERG blocker desipramine (11) and describe here in detail how desipramine inhibits hERG surface expression. We find a previously unrecognized combination of two independent mechanisms; desipramine 1) increases hERG endocytosis and degradation as a consequence of drug-induced channel ubiquitination and 2) rapidly inhibits hERG forward trafficking from the ER.

Based on Western analysis, electrophysiological current recordings, and immunocytochemical analysis, we have shown that hERG channels are rapidly removed from the cell surface upon desipramine exposure. Furthermore, hERG internalization was attenuated by dynasore, an inhibitor of dynamin that is crucial for the endocytosis of many surface proteins, *e.g.* via clathrin-coated vesicles (39). In addition, dynamin has also been implicated in several clathrin-independent endocytosis pathways including caveolae-associated mechanisms, which is of interest because hERG endocytosis induced under conditions of low $[K^+]_{ex}$ or in the presence of probucol appears to be linked to caveolin turnover (39–41). Although we do not address the precise endocytic mechanism(s) in our study, we note that inhibition of dynamin did not affect hERG surface expression under control conditions. One explanation may be that a dynamin-independent mechanism is at play in the absence of desipramine.

Importantly, the pronounced stability of fully glycosylated cell surface hERG does not imply that channels remain immobile at the cell surface. Instead, they undergo rapid, constitutive endocytic recycling, as has been described for several other cardiac potassium channels (35, 42). Under control conditions, about 20% of cell surface hERG was internalized within 1 h, with 80% of all internalized channels reappearing at the cell surface within minutes. Thus, we estimate that only about 4% of recycling hERG channels will be permanently lost from the cell surface via cellular degradation pathways over a time period of 1 h. Interestingly, in the presence of desipramine, hERG channels did not accumulate in the cell interior, as judged from our internalization assay, and channel recycling was unaffected. This strongly suggests that desipramine did not impair endocytic channel recycling in a nonspecific manner, *e.g.* via inhibition of calmodulin, which is thought to be involved in basal endocytic recycling processes (43–45), or via accumulation of

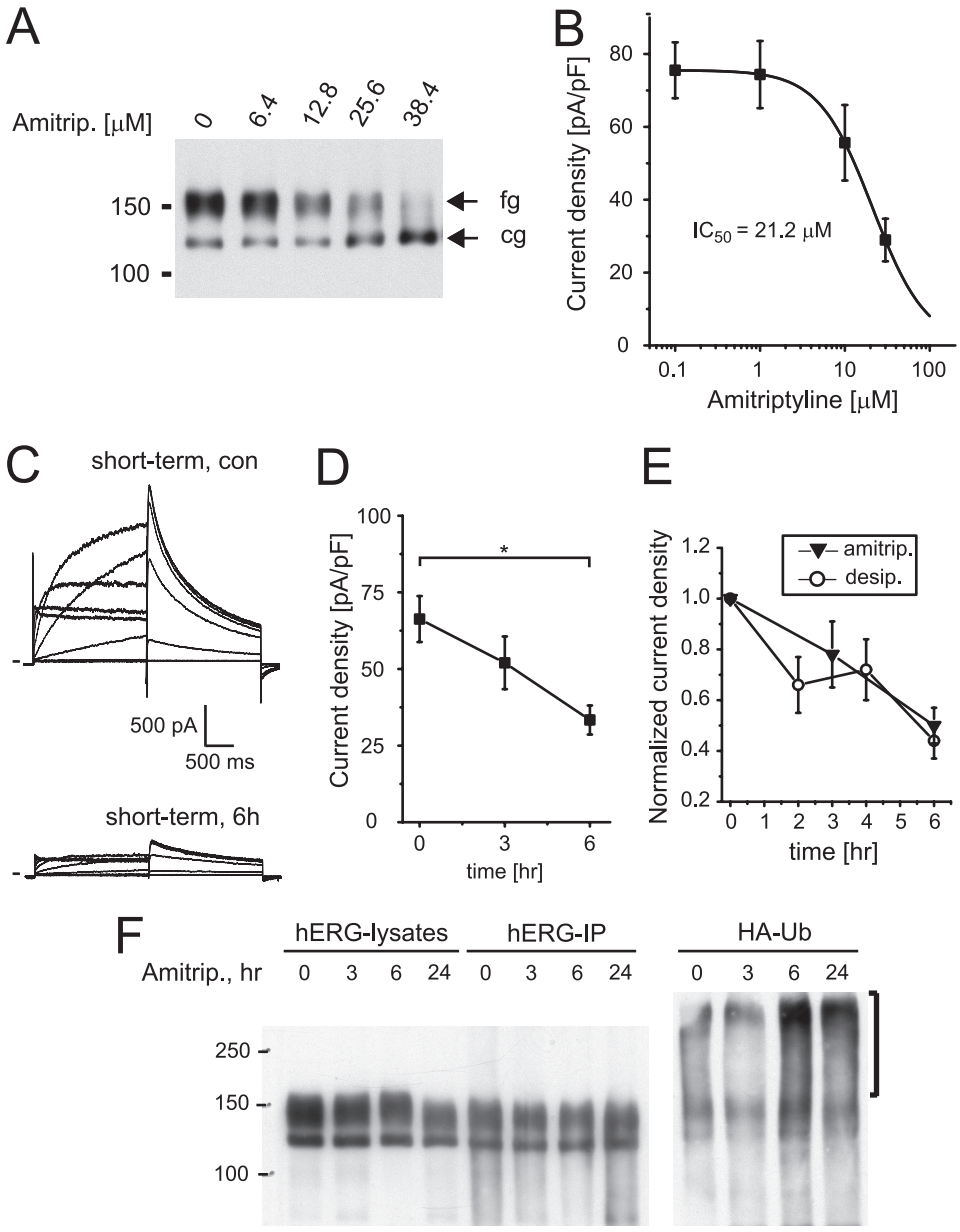

FIGURE 13. **Amitriptyline increases hERG ubiquitination.** *A*, Western blot shows the effects of overnight incubation with increasing concentrations of amitriptyline on hERG protein stably expressed in HEK293 cells. Equal amounts of protein were loaded; *fg* indicates the fully glycosylated, 150-kDa cell surface form of hERG; *cg* indicates the core-glycosylated, 135-kDa ER-resident form of hERG. *B*, shown are the concentration-dependent effects on hERG tail currents after overnight exposure to amitriptyline. IC_{50} is 21.2 μM ($n = 7$–13). *C*, representative hERG current families recorded under control conditions or after a 6-h exposure to 30 μM amitriptyline are shown. Currents were elicited using depolarizing voltage steps from −60 to +60 mV. Tail currents were recorded on return to −50 mV. Holding potential was −80 mV. *D*, time-dependent reduction of hERG tail current densities recorded on exposure to 30 μM amitriptyline ($n = 9$–10) is shown. Note that current density at $t = 6$ h is significantly different from control, Dunnett's, $p < 0.05$. *E*, normalized time-dependent changes in tail current levels recorded in the presence of either 30 μM desipramine or 30 μM amitriptyline (*amitrip*) are shown. *F*, shown is a Western blot analysis of HEK/hERG cells transiently transfected with HA-tagged ubiquitin and treated for 3 and 6 h or overnight (24 h) with 30 μM amitriptyline. Whole cell lysates, shown in the *right part of panel*, were immunoprecipitated with anti-hERG antibody, resolved by SDS-PAGE, and immunoblotted using either anti-hERG antibody (*hERG-IP*) or an antibody recognizing the HA epitope fused to ubiquitin (*HA-Ub*). Immunoblotting with anti-HA antibody identifies high molecular weight forms of ubiquitinated hERG that are increased on 6- and 24-h exposure to 30 μM desipramine. Data are given as the mean ± S.E.

cationic amphiphilic desipramine in acidic vesicular compartments, where it may disturb organelle pH (lysosomotropic drug action; Ref. 46). Intact cellular recycling pathways were also demonstrated by our observation that Kv1.5 as well as bEAG cell surface expression was not affected by desipramine exposure.

Because basal endocytic recycling is intact in the presence of desipramine, the question remained as to how hERG channels were removed from the cell surface upon drug exposure? We found that fully glycosylated hERG channels were rapidly and specifically multi-ubiquitinated in the presence of desipramine. Consequently, hERG channels were shifted toward higher molecular weight forms and were no longer detectable either on conventional Western blots or in internalization assays. It remains unclear whether channels are ubiquitinated at the cell surface or in an intracellular compartment. However, our experiments with dynasore suggest that ubiquitination most likely takes place in an intracellular compartment because fully

glycosylated hERG accumulated in a functional form at the cell surface on exposure to a combination of dynasore and desipramine. It is also not clear as to how hERG ubiquitination is initiated in the presence of desipramine? One possibility may be that desipramine is disturbing cholesterol-rich membranes (47). This could be deleterious to hERG channels that are thought to localize to cholesterol-rich lipid rafts (48). A similar hypothesis has been proposed to explain how probucol, a drug known to deplete cellular cholesterol levels, may induce hERG endocytosis (41). On the other hand, hERG endocytosis cannot be induced by exposure to methyl-β-cyclodextrin, a chelator often used to extract cholesterol from cell membranes (49).[3] Alternatively, desipramine may bind directly to hERG, thereby altering its conformation. However, should such a binding site exist, it must be distinct from the universal drug binding site of hERG in the conduction pathway, because mutation of residues within this site does not attenuate desipramine effects on hERG surface expression (11). This is in marked contrast to what has been reported for Kv1.5, where drug-induced endocytosis was initiated via binding of the blocker quinidine to the conduction pathway of Kv1.5 (50).

Once ubiquitinated, ion channels are degraded either via proteasomal or lysosomal pathways. Our data suggested lysosomal degradation, particularly in experiments with the lysosomal inhibitor bafilomycin, which was able to rescue fully glycosylated hERG on Western blots in the presence of desipramine. Although protein ubiquitination is commonly associated with proteasomal degradation, in many instances the addition of ubiquitin directs proteins toward lysosomal degradation, particularly with substrates that recycle along endocytic pathways. Examples are the β2-adrenergic receptor, the chemokine receptor CXCR4, or GABA(A) receptors (51, 52). Importantly, bafilomycin was not able to restore functional channels to the cell surface. This is similar to what has been described on exposure of hERG expressing cells to low potassium, where bafilomycin appears to arrest internalized hERG at the level of multivesicular bodies (53). Nevertheless, there were important differences between low potassium- and desipramine-induced hERG endocytosis. For example, direct channel ubiquitination was not unequivocally demonstrated under low potassium conditions. Moreover, in marked contrast to low potassium effects desipramine-induced hERG, internalization could not be reversed with proteasomal inhibitors (33).

In addition, desipramine was unique in that effects on channel endocytosis were accompanied by rapid inhibition of hERG forward trafficking as shown in pulse-chase experiments. We feel strongly that a reduction in fully glycosylated hERG, as seen in pulse-chase experiments, represents failure of ER export because export pathways that would bypass the Golgi have not been described for hERG and are unlikely to arise in the presence of desipramine as judged from our immunocytochemical analysis. However, important questions remain with respect to the precise mechanism(s) underlying ER retention that need to be addressed in future experiments. Importantly, desipramine did not affect crucial hERG-chaperone associations. Although surprising, this was consistent with observations that trafficking could not be restored with the pharmacological chaperone astemizole, which is thought to correct a wide range of conformational trafficking defects in hERG (38). A wide-ranging shutdown of all ER export appears also unlikely because cardiac action potentials were preserved, and neither Kv1.5 nor bEAG surface expression was affected on long term exposure to desipramine. Thus, we propose that desipramine may induce aggregation of near-native hERG channels in the ER. As a direct consequence, aggregated channels may be ubiquitinated and degraded. The proposed mechanism may also underlie fast ubiquitination of cell surface channels and provide a common link for simultaneous changes in channel endocytosis and forward trafficking as observed on drug exposure (54).

Taken together, we have described the first example of drug-induced channel ubiquitination and degradation with direct relevance for the cardiac safety of therapeutic compounds. Based on our data with amitriptyline and amoxapine, we speculate that the mechanisms described here for desipramine represent a class effect of all tri- and tetracyclic antidepressants. It seems that a combination of increased endocytosis, inhibition of forward trafficking, and acute hERG block could be clinically particularly worrisome, especially in the context of overdosing and intoxications. Collectively, our data clearly elucidate why TCAs are notorious for torsade de pointes arrhythmias and sudden cardiac death. Furthermore, it is conceivable that the mechanisms described here for TCAs may also apply to structurally closely related phenothiazine anti-psychotics such as thioridizine, trifluoperazine, or chlorpromazine, all of which are known to block hERG and reduce its surface expression at the same time (7). Finally, our data raise the important question of whether low affinity hERG blockers such as TCAs should not by all means be tested for possible effects on hERG surface expression, because acute block and chronic surface expression changes appear to operate in one and the same concentration window. Thus, focusing exclusively on the preclinical assessment of acute hERG blockade may underestimate the "true" cardiotoxicity of compounds with multiple effects on hERG.

[3] E. Ficker, unpublished data.

REFERENCES

1. Kannankeril, P., Roden, D. M., and Darbar, D. (2010) *Pharmacol. Rev.* **62,** 760–781
2. Sanguinetti, M. C., and Tristani-Firouzi, M. (2006) *Nature* **440,** 463–469
3. Ficker, E., Kuryshev, Y. A., Dennis, A. T., Obejero-Paz, C., Wang, L., Hawryluk, P., Wible, B. A., and Brown, A. M. (2004) *Mol. Pharmacol.* **66,** 33–44
4. Kuryshev, Y. A., Ficker, E., Wang, L., Hawryluk, P., Dennis, A. T., Wible, B. A., Brown, A. M., Kang, J., Chen, X. L., Sawamura, K., Reynolds, W., and Rampe, D. (2005) *J. Pharmacol. Exp. Ther.* **312,** 316–323
5. Cordes, J. S., Sun, Z., Lloyd, D. B., Bradley, J. A., Opsahl, A. C., Tengowski, M. W., Chen, X., and Zhou, J. (2005) *Br. J. Pharmacol.* **145,** 15–23
6. Dennis, A., Wang, L., Wan, X., and Ficker, E. (2007) *Biochem. Soc. Trans.* **35,** 1060–1063
7. Wible, B. A., Hawryluk, P., Ficker, E., Kuryshev, Y. A., Kirsch, G., and Brown, A. M. (2005) *J. Pharmacol. Toxicol. Methods* **52,** 136–145
8. Rajamani, S., Eckhardt, L. L., Valdivia, C. R., Klemens, C. A., Gillman, B. M., Anderson, C. L., Holzem, K. M., Delisle, B. P., Anson, B. D., Makielski, J. C., and January, C. T. (2006) *Br. J. Pharmacol.* **149,** 481–489
9. Takemasa, H., Nagatomo, T., Abe, H., Kawakami, K., Igarashi, T., Tsurugi, T., Kabashima, N., Tamura, M., Okazaki, M., Delisle, B. P., January, C. T., and Otsuji, Y. (2008) *Br. J. Pharmacol.* **153,** 439–447

10. Obers, S., Staudacher, I., Ficker, E., Dennis, A., Koschny, R., Erdal, H., Bloehs, R., Kisselbach, J., Karle, C. A., Schweizer, P. A., Katus, H. A., and Thomas, D. (2010) *Naunyn Schmiedebergs Arch. Pharmacol.* **381,** 385–400
11. Staudacher, I., Wang, L., Wan, X., Obers, S., Wenzel, W., Tristram, F., Koschny, R., Staudacher, K., Kisselbach, J., Koelsch, P., Schweizer, P. A., Katus, H. A., Ficker, E., and Thomas, D. (2011) *Naunyn Schmiedebergs Arch. Pharmacol.* **383,** 119–139
12. Pollard, C. E., Abi Gerges, N., Bridgland-Taylor, M. H., Easter, A., Hammond, T. G., and Valentin, J. P. (2010) *Br. J. Pharmacol.* **159,** 12–21
13. Witchel, H. J., Hancox, J. C., and Nutt, D. J. (2003) *J. Clin. Psychopharmacol.* **23,** 58–77
14. Ray, W. A., Meredith, S., Thapa, P. B., Hall, K., and Murray, K. T. (2004) *Clin. Pharmacol. Ther.* **75,** 234–241
15. Pull, C. B., and Damsa, C. (2008) *Neuropsychiatr. Dis. Treat.* **4,** 779–795
16. Jackson, J. L., Shimeall, W., Sessums, L., Dezee, K. J., Becher, D., Diemer, M., Berbano, E., and O'Malley, P. G. (2010) *BMJ* **341,** c5222
17. Dworkin, R. H., O'Connor, A. B., Audette, J., Baron, R., Gourlay, G. K., Haanpaa, M. L., Kent, J. L., Krane, E. J., Lebel, A. A., Levy, R. M., Mackey, S. C., Mayer, J., Miaskowski, C., Raja, S. N., Rice, A. S., Schmader, K. E., Stacey, B., Stanos, S., Treede, R. D., Turk, D. C., Walco, G. A., and Wells, C. D. (2010) *Mayo Clin. Proc.* **85,** S3–S14
18. Carter, W. P., Hudson, J. I., Lalonde, J. K., Pindyck, L., McElroy, S. L., and Pope, H. G., Jr. (2003) *Int. J. Eat. Disord.* **34,** S74–S88
19. Teschemacher, A. G., Seward, E. P., Hancox, J. C., and Witchel, H. J. (1999) *Br. J. Pharmacol.* **128,** 479–485
20. Kiesecker, C., Alter, M., Kathöfer, S., Zitron, E., Scholz, E. P., Thomas, D., Kreuzer, J., Katus, H. A., Bauer, A., and Karle, C. A. (2006) *Naunyn-Schmiedebergs Arch. Pharmacol.* **373,** 212–220
21. Hong, H. K., Park, M. H., Lee, B. H., and Jo, S. H. (2010) *Biochem. Biophys. Res. Commun.* **394,** 536–541
22. Hursting, M. J., Clark, G. D., Raisys, V. A., Miller, S. J., and Opheim, K. E. (1992) *Clin. Chem.* **38,** 2468–2471
23. Casazza, F., Fiorista, F., Rustici, A., and Brambilla, G. (1986) *G. Ital. Cardiol.* **16,** 1058–1061
24. Alderton, H. R. (1995) *Can. J. Psychiatry* **40,** 325–329
25. Leonard, H. L., Meyer, M. C., Swedo, S. E., Richter, D., Hamburger, S. D., Allen, A. J., Rapoport, J. L., and Tucker, E. (1995) *J. Am. Acad. Child Adolesc. Psychiatry* **34,** 1460–1468
26. Swanson, J. R., Jones, G. R., Krasselt, W., Denmark, L. N., and Ratti, F. (1997) *J. Forensic Sci.* **42,** 335–339
27. Waslick, B. D., Walsh, B. T., Greenhill, L. L., Giardina, E. G., Sloan, R. P., Bigger, J. T., and Bilich, K. (1999) *J. Am. Acad. Child Adolesc. Psychiatry* **38,** 179–186
28. Varley, C. K. (2001) *Paediatr. Drugs* **3,** 613–627
29. Ficker, E., Dennis, A. T., Wang, L., and Brown, A. M. (2003) *Circ. Res.* **92,** e87–100
30. Kirchhausen, T., Macia, E., and Pelish, H. E. (2008) *Methods Enzymol.* **438,** 77–93
31. Zhang, S. (2006) *Am. J. Physiol. Heart Circ. Physiol.* **290,** H1038–H1049
32. Falcón-Pérez, J. M., Nazarian, R., Sabatti, C., and Dell'Angelica, E. C. (2005) *J. Cell Sci.* **118,** 5243–5255
33. Guo, J., Massaeli, H., Xu, J., Jia, Z., Wigle, J. T., Mesaeli, N., and Zhang, S. (2009) *J. Clin. Invest.* **119,** 2745–2757
34. Choi, W. S., Khurana, A., Mathur, R., Viswanathan, V., Steele, D. F., and Fedida, D. (2005) *Circ. Res.* **97,** 363–371
35. McEwen, D. P., Schumacher, S. M., Li, Q., Benson, M. D., Iñiguez-Lluhí, J. A., Van Genderen, K. M., and Martens, J. R. (2007) *J. Biol. Chem.* **282,** 29612–29620
36. Zadeh, A. D., Xu, H., Loewen, M. E., Noble, G. P., Steele, D. F., and Fedida, D. (2008) *J. Physiol.* **586,** 4793–4813
37. Silvis, M. R., Bertrand, C. A., Ameen, N., Golin-Bisello, F., Butterworth, M. B., Frizzell, R. A., and Bradbury, N. A. (2009) *Mol. Biol. Cell* **20,** 2337–2350
38. Ficker, E., Obejero-Paz, C. A., Zhao, S., and Brown, A. M. (2002) *J. Biol. Chem.* **277,** 4989–4998
39. Doherty, G. J., and McMahon, H. T. (2009) *Annu. Rev. Biochem.* **78,** 857–902
40. Massaeli, H., Sun, T., Li, X., Shallow, H., Wu, J., Xu, J., Li, W., Hanson, C., Guo, J., and Zhang, S. (2010) *J. Biol. Chem.* **285,** 27259–27264
41. Guo, J., Li, X., Shallow, H., Xu, J., Yang, T., Massaeli, H., Li, W., Sun, T., Pierce, G. N., and Zhang, S. (2011) *Mol. Pharmacol.* **79,** 806–813
42. Seebohm, G., Strutz-Seebohm, N., Birkin, R., Dell, G., Bucci, C., Spinosa, M. R., Baltaev, R., Mack, A. F., Korniychuk, G., Choudhury, A., Marks, D., Pagano, R. E., Attali, B., Pfeufer, A., Kass, R. S., Sanguinetti, M. C., Tavare, J. M., and Lang, F. (2007) *Circ. Res.* **100,** 686–692
43. Prozialeck, W. C., and Weiss, B. (1982) *J. Pharmacol. Exp. Ther.* **222,** 509–516
44. Apodaca, G., Enrich, C., and Mostov, K. E. (1994) *J. Biol. Chem.* **269,** 19005–19013
45. Colombo, M. I., Beron, W., and Stahl, P. D. (1997) *J. Biol. Chem.* **272,** 7707–7712
46. Honegger, U. E., Roscher, A. A., and Wiesmann, U. N. (1983) *J. Pharmacol. Exp. Ther.* **225,** 436–441
47. Pakkanen, K., Salonen, E., Mäkelä, A. R., Oker-Blom, C., Vattulainen, I., and Vuento, M. (2009) *Phys. Biol.* **6,** 046004
48. Balijepalli, R. C., Delisle, B. P., Balijepalli, S. Y., Foell, J. D., Slind, J. K., Kamp, T. J., and January, C. T. (2007) *Channels* **1,** 263–272
49. Christian, A. E., Haynes, M. P., Phillips, M. C., and Rothblat, G. H. (1997) *J. Lipid Res.* **38,** 2264–2272
50. Schumacher, S. M., McEwen, D. P., Zhang, L., Arendt, K. L., Van Genderen, K. M., and Martens, J. R. (2009) *Circ. Res.* **104,** 1390–1398
51. Shenoy, S. K. (2011) *Curr. Top. Membr.* **67,** 51–78
52. Arancibia-Cárcamo, I. L., Yuen, E. Y., Muir, J., Lumb, M. J., Michels, G., Saliba, R. S., Smart, T. G., Yan, Z., Kittler, J. T., and Moss, S. J. (2009) *Proc. Natl. Acad. Sci. U.S.A.* **106,** 17552–17557
53. Sun, T., Guo, J., Shallow, H., Yang, T., Xu, J., Li, W., Hanson, C., Wu, J. G., Li, X., Massaeli, H., and Zhang, S. (2011) *J. Biol. Chem.* **286,** 6751–6759
54. Liu, A. P., Aguet, F., Danuser, G., and Schmid, S. L. (2010) *J. Cell Biol.* **191,** 1381–1393